



Cite this: *Soft Matter*, 2025,
21, 5862

Fredericksz transitions in the nematic and smectic Z_A phases of DIO[†]

J. T. Gleeson, ^{*a} S. N. Sprunt, ^a A. Jákli, ^{ab} P. Guragain ^c and R. J. Twieg ^c

The remarkable material DIO presents fascinating behaviors. It has been extensively studied as one of the first materials exhibiting a ferroelectric nematic phase. However, at higher temperatures it exhibits what has been termed the smectic Z_A : identified as an orientationally ordered, antiferroelectric phase with a density modulation in direction perpendicular to the optic axis. At even higher temperatures, this transitions to an apparently normal nematic phase. We have studied the splay-bend Fredericksz transition in the nematic and SmZ_A phases of the material DIO. Both the magnetic and electric field transitions were utilized. We observed the transitions by measuring effective birefringence and capacitance as well as with polarizing light microscopy. In both the nematic and the SmZ_A states the field induced transitions resemble (in numerous aspects) the classical Fredericksz transition. These enable determinations of several fundamental material parameters and also reveal intriguing aspects of the SmZ_A phase, including the surprising behavior of the elastic constants and the dielectric anisotropy. Detailed comparison with Frank elastic theory of the Fredericksz transition shows that the N phase behaves largely as expected, but the transition in the SmZ_A phase differs significantly. Two specific examples of this are the onset of striations in the Fredericksz distorted state, and the presence of optical biaxiality. The former may be related to the periodic Fredericksz transition as it coincides with a large increase in the splay elastic constant. The latter has been predicted for the SmZ_A phase, but not previously observed.

Received 6th March 2025,
Accepted 11th June 2025

DOI: 10.1039/d5sm00238a

rsc.li/soft-matter-journal

Introduction

The behavior of nematic liquid crystals (NLC) under external electric and/or magnetic fields is extremely well studied. Indeed, using an electric field to control the optical axis of a NLC underpins the overwhelming majority of NLC technologies. This enormous body of work provides a useful framework with which we can place the new liquid crystal mesophases, such as the smectic Z_A (SmZ_A) studied here, into context.⁴ More specifically, the Fredericksz transition (FT),^{5,6} in which the orienting effects of confining substrates are in opposition to the effect of an external field, has been exhaustively examined, both theoretically and experimentally. The “classical” FT is characterized by a non-zero threshold field at which the optic axis begins to rotate away from its zero-field state. Upon extrapolating the field to infinite strength, the optic axis becomes parallel to the field direction.

This work presents a detailed study of both the electric and magnetic field induced FT in the of the material DIO.⁷ This material, in addition to exhibiting the polar, ferroelectric nematic (N_F) phase (which is not the topic of this work) also exhibits both the uniaxial, apolar nematic (N) phases and the newly described smectic Z_A (SmZ_A) phase.³ Both the N and SmZ_A exhibit both electric and magnetic field induced FT's. All transitions are qualitatively similar, although the differences are both important and illuminating. Tracking how these transitions evolve as the material progresses between the two phases brings this into even sharper focus.

In particular, we focus on the splay-bend FT,⁵ in which a LC is confined between parallel plates separated by a distance, d . The plates are treated so as to induce uniform surface alignment (defined as the x direction). Because of the anisotropy in either the dielectric tensor or the diamagnetic susceptibility tensor, an external field exerts a torque on the LC director. When the applied field exceeds its threshold, the director rotates in the z direction.

For the magnetic case, the threshold field is $B_c = \frac{\pi}{d} \sqrt{\frac{K_{11}\mu_0}{\Delta\chi}}$, where K_{11} is the splay elastic constant, μ_0 is the permittivity of free space, $\Delta\chi$ is the anisotropy in the diamagnetic susceptibility. Thus, studying this transition yields important information on the balance between elastic and external field effects. There is copious literature on every aspect of this effect.^{1,8}

^a Department of Physics, Kent State University, Kent, OH 44242, USA.
E-mail: jgleeson@kent.edu

^b Materials Science Graduate Program and Advanced Materials and Liquid Crystal Institute, Kent State University, Kent, OH 44242, USA

^c Department of Chemistry and Biochemistry, Kent State University, Kent, OH 44242, USA

[†] Electronic supplementary information (ESI) available. See DOI: <https://doi.org/10.1039/d5sm00238a>



How will the SmZ_A phase be affected by external fields? Two attributes of the SmZ_A phase can be expected to be significant. In addition to the elastic energy modes associated with distorting the nematic director, we can anticipate there will be additional modes involving distortion of the layered structure. Moreover, as is common in all smectic phases, modes which would require layer compression or dilation should be forbidden. That is, any director mode that requires rotation out of the layer plane, or which would necessitate layer rupture is therefore strongly suppressed. At present, there is no comprehensive description of the elastic energy of the SmZ_A phase. Furthermore, the antiferroelectric nature of the SmZ_A phase in DIO cannot be neglected. While antiferroelectric materials have no net polarization at zero applied electric field, they should be substantially more polarizable than the nematic phase. Because of this, we might anticipate the coupling to an applied electric field to be rather more complex than the well-known director torque *via* the anisotropy in the dielectric constants.

Experiments

The material DIO⁹ (2,3',4',5'-tetrafluoro[1,1'-biphenyl]-4-yl 2,6-difluoro-4-(5-propyl-1,3-dioxan-2-yl)benzoate was resynthesized¹⁰ as described in ESI.† Its purity was confirmed using NMR and DSC; moreover, all phase transitions as described below were sharp, well-defined and in agreement with published values.¹¹ This compound has two stereo isomers, and at elevated temperatures, isomerization may take place.¹² As described in the ESI,† we used isomerically pure (*trans*) DIO, and took care to never heat it above 100 °C. Using this material, we filled sandwich cells having rubbed polyimide surface treatment to create planar alignment. Before filling, the plate separation, *d*, was measured interferometrically, and the capacitance of the empty cell recorded. Cells were filled using capillary action at 100 °C on a hotplate. We observed uniform planar alignment in both the N and SmZ_A phases of DIO.

With planar alignment, the splay-bend Freedericksz transition (FT)⁵ is possible using an external field perpendicular to the alignment direction (and hence the substrates). We explored this using both ac electric field (at various frequencies) and dc magnetic field. Furthermore, as this FT corresponds to an increase of the angle between the director and the planar aligning surfaces (θ), we employed three complementary probes to detect and monitor this director distortion: capacitance, optical phase difference and microscopy.

For all measurements, the samples were held in a temperature-controlled enclosure. As previously noted, we took pains that the sample temperature never exceeded 100 °C. The capacitance (and loss) of the material was determined by applying a sinusoidal voltage of varying frequency and amplitude between the ITO electrodes and measuring the in-phase and out-of-phase current. For this we used a variable gain current-to-voltage pre-amplifier. Before making any measurements, the NLC cell was substituted for purely resistive load and the lock-in amplifier phase angle adjusted so that the out-of-phase

current registered at zero. This step eliminates the influence of residual capacitance in lead wires, *etc*. The entire circuit was then tested using a standard capacitor. With this arrangement we can measure the capacitance and loss of the LC sample subject to a sinusoidal potential difference having amplitude varying between 0.004 V_{rms} and 5 V_{rms}, and with frequency between 10 Hz and 50 kHz.

In order to study the magnetic field induced Freedericksz transition, the LC sample was suspended in the bore of a 10 T superconducting solenoid. For these experiments, the magnetic field direction was perpendicular to the glass plates (and the alignment direction). With this we can measure the capacitance (and loss) of the LC layer at various magnetic fields. Furthermore, the housing had a 2 mm through hole for optical access. By positioning a lamp and a polarizer inside the magnet, and with use of a long-distance, reflecting microscope we could obtain polarizing optical microscopy images of the LC layer subject to magnetic fields. However, the constraints of the magnet and the vibrations of the cooling system limited both the magnification and resolution.

In addition to the above, we also performed optical phase difference (OPD) measurements for the electric-field induced Freedericksz transition. For these we employed the standard photo-elastic modulator technique,¹³ with additional phase compensation to establish the zero OPD configuration.

Results

In order to understand the baseline of field induced effects in this material, we begin with a comprehensive investigation of the nematic phase in DIO. Prior to any measurements, the textures of the samples were examined using polarized optical microscopy (POM). In all cases, uniform, planar alignment was observed throughout both the N and the SmZ_A phases. Indeed, the transition from N to SmZ_A is rather subtle as observed in the microscope, as has been previously reported.³

A sandwich cell with planar alignment corresponds to the nematic director perpendicular to the substrate normal (with no applied field). Before filling with DIO, the capacitance of the empty cell, $C_0 = \frac{\epsilon_0 A}{d}$, where *A* is the electrode area, *d* is electrode separation was measured. Therefore, the measured capacitance is given by $C = \frac{\epsilon_{\perp} \epsilon_0 A}{d}$ when *V*₀, the potential difference used to make the measurements is small. The ratio C/C_0 then yields ϵ_{\perp} . Fig. 1 shows ϵ_{\perp} vs. temperature at a variety of different frequencies. Both the N-SmZ_A and the SmZ_A-N_F transitions are prominent. The values shown for the N_F phase were based upon the capacitance as actually measured. We note that there are unresolved issues concerning this;¹⁴ however these are not within the scope of the present paper. We do not represent that values shown here below the SmZ_A-N_F transition temperature are reflective of the N_F state.

We examined both the magnetic field and electric field FT in the nematic phase of DIO. Note that these studies do not span the entire nematic phase range, as we took cautions to remain



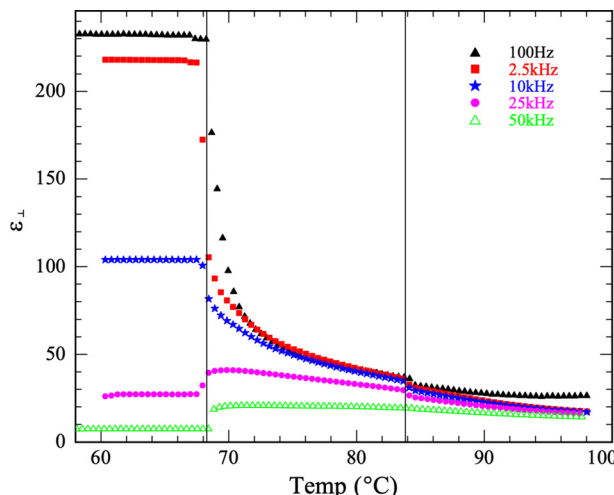


Fig. 1 Perpendicular component of dielectric constant vs. temperature at various frequencies. The vertical lines indicate the N–SmZ_A and the SmZ_A–N_F phase transitions.

below 100 °C as described above. Both effects were studied *via* measurement of capacitance, and the electric-field induced FT was also studied *via* OPD measurement. In all cases we waited at least one second between data points; this was found to be much longer than any transients after a change in applied field. In order to verify that this was sufficiently long, we repeated several scans using double the waiting time; no difference was observed between these two cases. We also obtained POM images of the texture during both transitions. In the nematic phase, we observe the classic Freedericksz transition. At voltages well below and well above the transition we observe a uniform texture. Frequently, as the voltage is increased above the threshold we temporarily observe walls.¹⁵ These disappear within a few seconds. While the electric field induced transition can be studied at frequencies ranging between 100 Hz–50 kHz, we selected a single frequency, 2.5 kHz for all Freedericksz transition measurements. This is because while the dielectric properties will depend on frequency, the elastic constants do not. This choice permits us to perform detailed studies comparing both magnetic and electric field induced transitions. Fig. 2 shows an example of how the effective birefringence, $n_{\text{eff}} - n_0$ depends on applied voltage.

Capacitance measurements are particularly valuable in studying the Freedericksz transition. The transition may be induced by the probe field, which can be of variable frequency. Moreover, the values measured both at very small external field (*i.e.* below the threshold) and, by extrapolating to infinite field reveal the perpendicular and parallel components of the dielectric tensor (ϵ_{\perp} and ϵ_{\parallel}), (at the desired frequency).¹⁶ The threshold FT voltage, given by $V_c = \pi \sqrt{\frac{K_{11}}{\epsilon_0 \Delta \epsilon}}$, which is straightforward to measure, yields the splay elastic constant. An example of capacitance measurements during the electric field induced FT is shown in Fig. 3. Lastly, an example of the capacitance during the magnetic field induced FT is shown in Fig. 4. In the nematic phase, both types of FT are useful for determining material

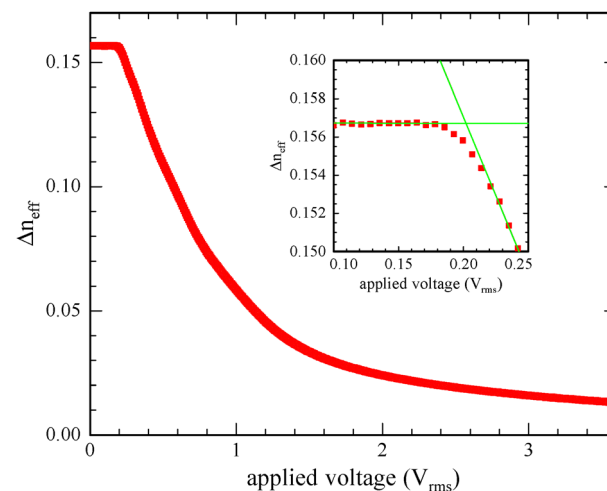


Fig. 2 Effective birefringence vs. applied voltage for DIO at 84 °C and 2.5 kHz. Inset shows close up of Freedericksz transition along with the fitting used to determine the threshold voltage.

parameters as described below. Specifically, if we plot these measurements in a reduced fashion, *i.e.* plotting $\frac{\epsilon_{\text{eff}}}{\epsilon_{\parallel}} - 1$ vs. $\frac{B}{B_c} - 1$ (or $\frac{V}{V_c} - 1$), elastic theory predicts the curve obtained should be linear right above the transition, having slope $\frac{2\gamma}{1+\kappa}$ (for the magnetic FT), where $\gamma = \frac{\epsilon_{\parallel}}{\epsilon_{\perp}} - 1$ and $\kappa = \frac{K_{33}}{K_{11}} - 1$. For the electric case, the slope will be $\frac{2\gamma}{1+\kappa+\gamma}$.^{8,16} Thus, with these two measurements we can obtain the dielectric anisotropy, the splay and bend elastic constants, and the diamagnetic anisotropy. The temperature dependence of both elastic constants is shown in Fig. 5. These

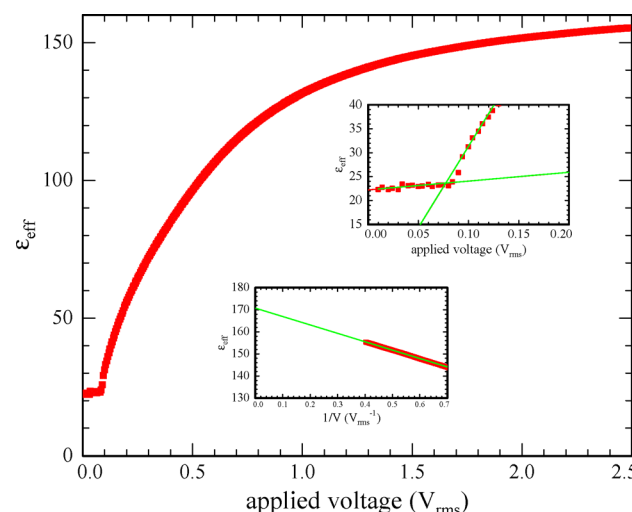


Fig. 3 Effective dielectric constant vs. voltage at 90 °C and 2.5 kHz. The upper inset shows the transition occurring at 0.076 V_{rms}. The lower inset shows the extrapolation to infinite voltage enabling the determination of ϵ_{\parallel} .



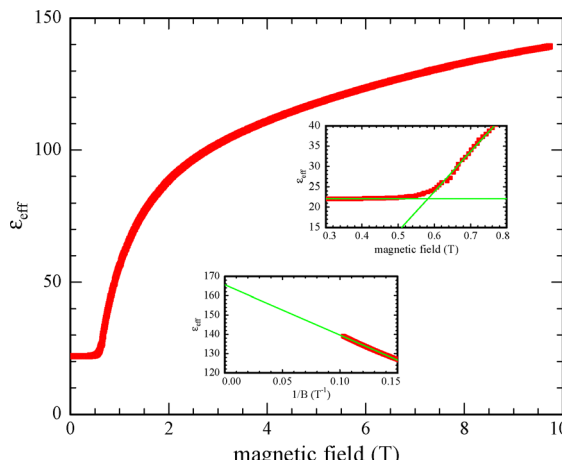


Fig. 4 Effective dielectric constant vs. magnetic field at 90 °C. The probe voltage is 0.004 V_{rms} at 2.5 kHz. Upper inset shows close-up of FT; lower inset shows extrapolation to infinite magnetic field.

results are comparable with ref. 12 where measurements solely in the N phase are reported.

The dynamics of the FT can yield insight into LC flow properties. Specifically, upon stepwise reduction of the external field (from above threshold to zero), the effective birefringence increases exponentially with time constant $\tau_0 = \frac{\gamma_1 d^2}{K_{11}\pi^2}$, where γ_1 is the orientational viscosity. Although backflow effects are expected in this geometry, their presence should not affect the time constant.¹⁷ An example of the birefringence relaxation is shown inset Fig. 6; the main figure shows the dependence of γ_1 on temperature. It is notable that while the viscosity increases as you enter the SmZ_A from the N phase, there is

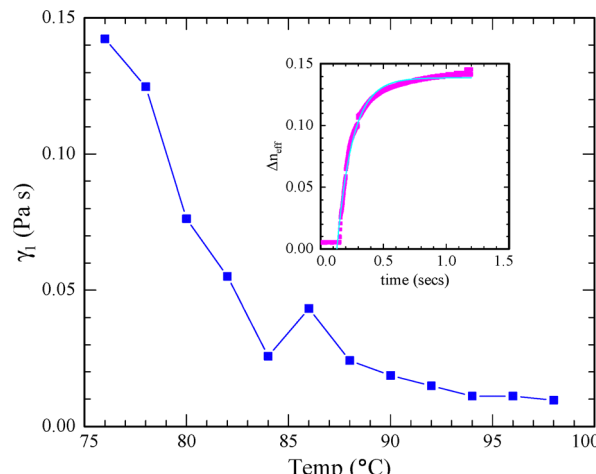


Fig. 6 Rotational viscosity vs. temperature. Inset: Example of change in effective birefringence vs. time after stepwise decrease in applied voltage. Green line shows fit to single exponential.

no abrupt change. Furthermore, and the values of γ_1 are not significantly different from calamitic nematic materials.

Ref. 3 posits that aligned samples of the SmZ_A phase will be biaxial, *i.e.* there will be some residual birefringence when the principal axis of the refractive index tensor is parallel to the optical wavevector. This is not surprising in that there are two distinct directions in the plane perpendicular to the director as this plane contains the layer normal. Nonetheless optical biaxiality in liquid crystals is typically difficult to measure.^{18,19} Our approach uses an external field to unambiguously align the principal optic axis and then test for residual birefringence in the plane perpendicular to it.^{20–22} Uniaxial materials should extrapolate to zero residual birefringence at infinite field, as in this case the single optic axis will be collinear with the field. However, this will only be strictly true in the case of infinite surface anchoring potential, which is certainly not the case in practice. In the case of finite surface anchoring,²³ the residual birefringence will reach zero at finite applied field, and so the extrapolated value will be negative; we can see this above the N-SmZ_A transition in Fig. 7. This figure clearly shows the onset and increase of biaxiality as one cools below the N-SmZ_A transition temperature.

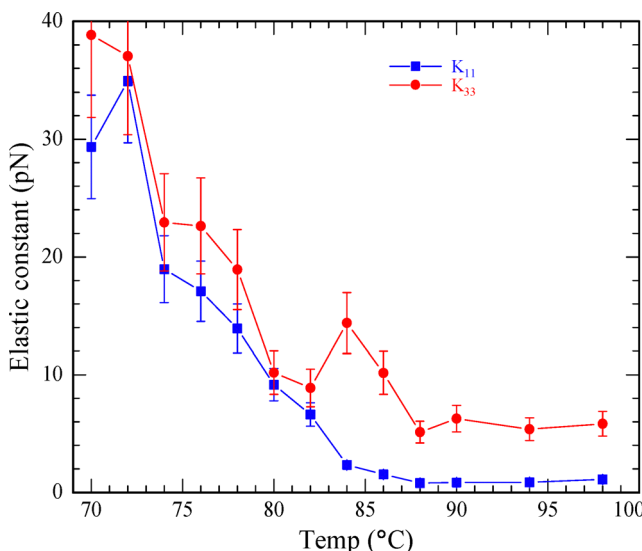


Fig. 5 Splay and bend elastic constants of DIO vs. temperature. Both increase dramatically at the N–SmZ_A transition. The error bars reflect the uncertainty in determining both the threshold potential difference and the slope at onset (for K33).

Discussion

The results above show that both (electric and magnetic) field induced splay-bend Freedericksz transitions occur in N and SmZ_A phases of DIO. The observations in the nematic phase are of course to be expected. In the SmZ_A phase it is less clear what is to be expected. It is instructive to look more closely at this transition, and to examine in detail how the both the transition and the distorted state above it differ as the material enters the SmZ_A phase from the nematic.

In the ideal FT, (*i.e.* infinite anchoring strength, zero pre-tilt angle), at the threshold field the measured quantity (capacitance or birefringence) will exhibit a discontinuity in its slope. When these assumptions are relaxed, the transition will



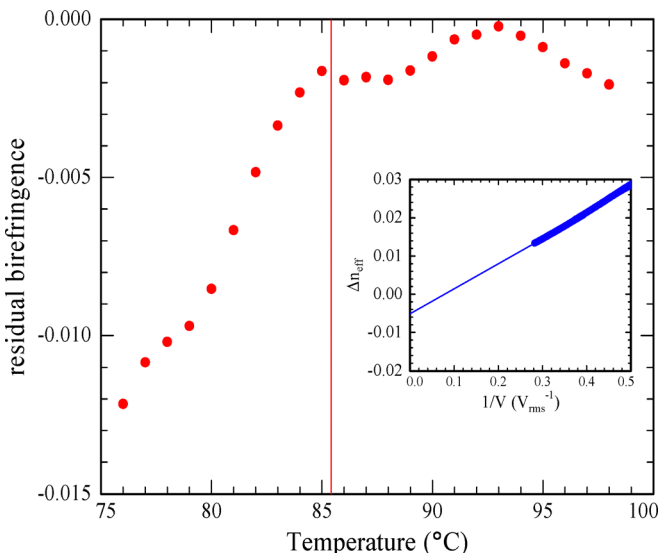


Fig. 7 Effective birefringence extrapolated to infinite potential difference vs. temperature. Vertical line is the N-SmZ_A transition. Inset: Extrapolation example (corresponds to 80 °C).

become rounded.^{24,25} In DIO, this is also observed, but the rounding becomes far more pronounced in the SmZ_A phase, as is shown in Fig. 9. While it is difficult to ascertain the exact cause for the enhanced rounding, it would seem unlikely that the onset of the SmZ_A is accompanied by a significant increase in pre-tilt angle. Moreover, were this the case, similar behavior would be seen in the magnetic FT. Fig. 8 shows that this is not the case. In other words, the origin of the dramatic rounding of the electrically induced transition is unclear. This effect also contributes to the uncertainty in determining the elastic constants, as is reflected in the error bars in Fig. 5.

The FT in DIO, especially in the SmZ_A phase, exhibits further discrepancies from the ideal, nematic FT. The standard Oseen-Frank theory for the FT predicts that at the threshold field there is an exchange of stability between the undistorted and the

distorted states. That is, right above the threshold the undistorted state is unstable, and right below the distorted state becomes unstable. Therefore, in the well-known nematic FT one expects no difference no matter whether the external field is increasing or decreasing, except perhaps if the field is changed more rapidly than the LC's ability to respond. This is indeed what is observed with DIO in the N phase, for both electric and magnetic fields. In the SmZ_A phase, we observe rather different behavior. An example of the magnetic FT is shown in Fig. 10. In this case we observe a 30% increase in the critical field depending on whether it is increasing or decreasing. The time frame for both of these scans is roughly one hour. An interesting but open question for further study concerns whether or not this hysteresis would remain if the measurement were done slowly enough. The overall curve is not substantially altered. In other words, the elastic resistance to the director distortion is lower (*i.e.* lower K_{11}) when the field is increased (from below to above threshold) than when the field is decreased. The electric FT in the SmZ_A phase is even more intriguing (see Fig. 9). In this case, the SmZ_A phase not only shows a difference in threshold voltage between increasing and decreasing, but the overall shape of the response is dramatically different. The transition is more rounded, and the initial slope is very different.

Indeed, the FT is not the only circumstance where hysteresis is observed, although it is the most prominent; Fig. 1 shows the dependence of ε_{\perp} on temperature. When this is examined more closely, comparing cooling from above the N-SmZ_A phase transitions to and heating from below the N_F-SmZ_A transition, N_F phase, a small but significant difference emerges, but only within the SmZ_A phase - *cf.* Fig. 11. We further note that no difference is discernible *via* POM comparing heating and cooling through the SmZ_A range. Possible origins of these hysteretic behaviors are discussed subsequently.

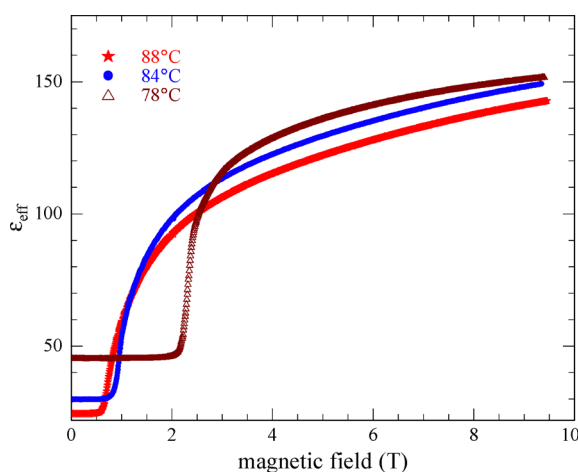


Fig. 8 Magnetic field induced FT at different temperatures above and below the N-SmZ_A transition. No significant increase in rounding is seen below the transition temperature.

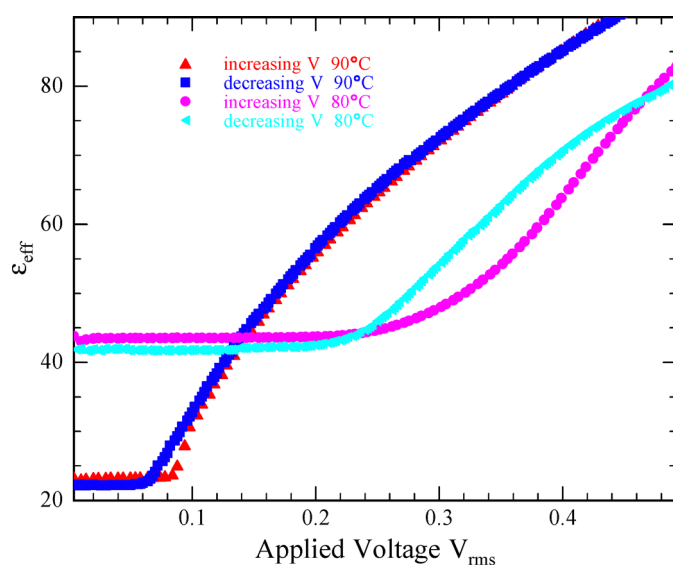


Fig. 9 Effective dielectric constants for both increasing and decreasing applied voltage in both the N and SmZ_A phase: frequency 2.5 kHz.



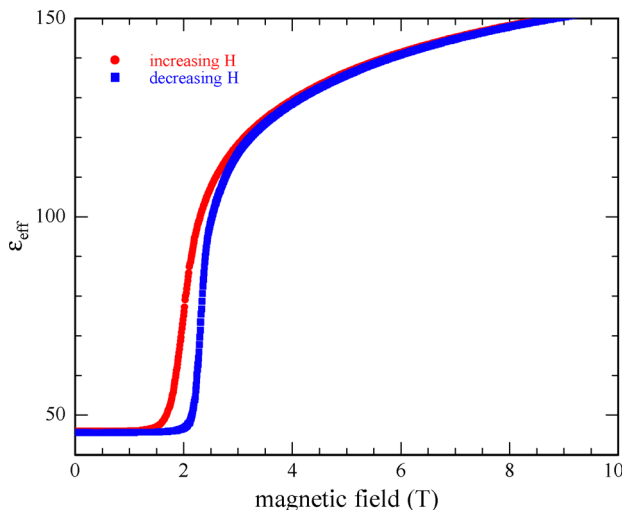


Fig. 10 Hysteresis of the magnetic FT in SmZ_A phase of DIO. Temperature 78 °C; probe voltage 0.004 V_{rms}; 2.5 kHz.

What is the origin of these hysteretic behaviors? In both the N and N_F phases, there is no hysteresis between heating and cooling; in the SmZ_A phase it is unmistakable and repeatable. In the N phase, during both electric and magnetic field-induced FT's, there are only minor differences between increasing and decreasing applied fields. These differences are common in traditional nematics, and usually disappear when the fields' rate-of-change is sufficiently low. This is not the case in the SmZ_A phase. In the magnetic FT, there is a persistent difference in the critical field between increasing and decreasing H. In the electric FT, not only is the critical voltage hysteretic, but there is also a distinct difference in the observed shape of the curve depending on direction.

Fig. 11 probes the component of the dielectric constant perpendicular to the nematic director, which is dictated by the planar surface alignment treatment on the glass plates.

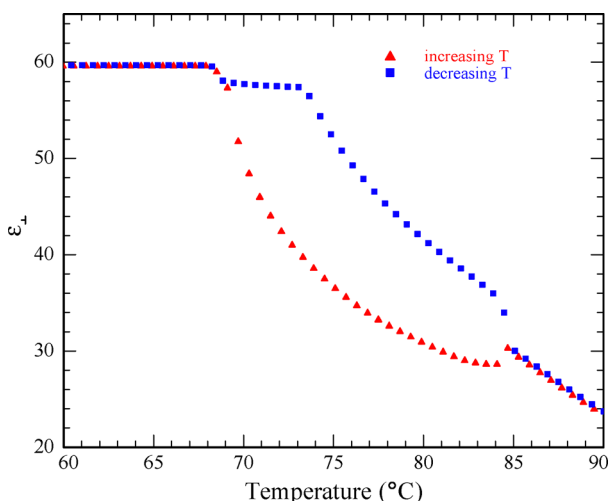


Fig. 11 Temperature dependence of ϵ_\perp during both heating and cooling. Measured at 10 kHz and probe voltage of 0.05 V_{rms}. Note the unusual kink at 73.3°C, but only during cooling.

Unspecified is the direction of the smectic layering in the SmZ_A state. Two extremes are imagined in ref. 3 in one the layer normal (which must be perpendicular to the director) lies in the plane of the glass plates (the “bookshelf” geometry); in the other the layer is perpendicular to the glass plates (the “parallel” geometry). Other than by X-ray scattering techniques, (which are not practical in thin film geometries), unambiguous determination of the layer normal direction is not possible. Moreover, by definition, a uniaxial material has two equal eigenvalues of the dielectric constant tensor, but a biaxial material, such as SmZ_A can have three distinct eigenvalues. While not definitive, we argue this is most straightforward explanation for the hysteresis observed in Fig. 11. That is, cooling from the N phase results in a different layering structure (but the same director orientation) than heating from the N_F phase. Ref. 3 presents evidence that upon cooling from N, the bookshelf geometry is favored over the parallel. While the data we present is consistent with a differing geometry depending on whether one cools from the N or heats from the N_F , it is more difficult to ascertain which is which. Lastly, during the cooling scan in Fig. 11, about 4 degrees above the N_F phase transition, a knee is observed (this is absent during heating). Below this knee ϵ_\perp does not change with temperature (as is seen in the N_F phase), so it seems logical that this is a pre-transitional effect, although its nature has not yet been determined.

Can the different layering geometries explain the hysteresis in the FT's? The magnetic case is more straightforward. If, below the transition (*i.e.* planar aligned director) the layers are bookshelf, the director distortion can commence without change in the layer normal. This is because in undistorted bookshelf the layer normal is the plane of the substrates. At very high field, the director becomes nearly homeotropic (*i.e.* perpendicular to the aligning surfaces). In this state, the layer normal will be degenerate in the plane of the aligning surfaces, *i.e.* not necessarily in the plane of the substrates. If this is the case, as the field is decreased, not only will the director be distorted, but also the layer normal. This additional distortion mode should increase the effective elastic constant leading to a larger critical field.

The preceding argument is more difficult to apply to the electric FT. This observation leads to a more significant indication. In the nematic phase, the electric and magnetic field induced FT's are essentially the same, other than a correction due to the electric susceptibility being so much larger than the magnetic. In the SmZ_A phase, there is clear evidence that the two Fredericksz transitions (electric and magnetic) are fundamentally, and qualitatively, different. What might explain such differing external field couplings? We argue the most likely cause by far is the anti-ferroelectric nature demonstrated for the SmZ_A phase in DIO.³ In addition, further interactions have been proposed, including competition between flexoelectricity and polar order (both ferroelectric and antiferroelectric).^{26,27} It remains to be seen whether or not this effect may be present and/or observable *via* the Fredericksz transition.

The most obvious difference between the magnetic and electric field induced transitions in the SmZ_A is the sharpness. In nematics, an ideal FT (infinite anchoring strength, zero



Fig. 12 POM image of DIO in SmZ_A phase right above threshold for magnetic FT. Periodic striations perpendicular to rubbing direction are observed (not seen in N phase).

pre-tilt) exhibits a discontinuity in slope. The transition shows rounding with either finite anchoring energy or pre-tilt (or both). How could these factors differentiate between magnetic and electric field? The antiferroelectric structure of SmZ_A comprises a persistent polarization along the director and alternating periodically. In both the bookshelf and parallel geometries, a non-zero pre-tilt angle (at zero applied field) gives a small component of polarization perpendicular to the substrates. This component will have a linear coupling to an applied electric field, but not to any magnetic field. Thus, for any non-zero pretilt, we would expect a difference between the electric and magnetic field induced transitions in the SmZ_A phase.

Above the FT threshold, there are intriguing implications of the dramatic increase in measured elastic constants in the SmZ_A phase seen in Fig. 5. As one enters the SmZ_A phase from the N phase, K_{11} and K_{33} both become much larger (reaching more than 30× their value in the N phase). Yet, the increase is gradual, not abrupt; moreover, the increase begins above the phase transition temperature. This is in contrast to the well-known behavior whereby when approaching the N-SmA transition, the twist and bend elastic constants diverge, as these distortions are forbidden in the SmA state as they cannot be decoupled from layer compression.⁶ Furthermore, in this case the divergence occurs in the higher temperature N phase; in the present case most of the increase is observed in the lower temperature SmZ_A phase.

Conclusions

When the cost of splay deformation becomes large, other manifestations of the Freedericksz transition may arise; in the most notable a periodic modulation arises in which twist deformation is substituted for splay.² Such modulations are expected when K_{11} is more than twice K_{22} . Since DIO exhibits a large increase in K_{11} , the possibility of the periodic FT must be considered. Indeed, Fig. 12 shows POM just above the magnetic field induced FT at 71 °C, where the splay constant is found to be 30 times its value in the N phase. There is clearly a modulated texture, although its periodicity appears to be poorly

defined. A modulated texture is also observed above the electric field induced FT, although the character and spacing of the modulations appears to be different. In addition, the periodic FT requires splay much larger than twist. While the splay constant does increase dramatically, and there are as yet no measurements of the twist constant, it is argued² that the SmZ_A layer structure precludes twist; it cannot be established that the periodic FT criteria are met in DIO. We lastly note a recent report of a periodic FT in the ferroelectric nematic state; while this work is in a related material, its origin is very different from what we report.

It is somewhat surprising that the SmZ_A phase exhibits field induced reorientation in a manner so similar to NLC materials. While measurements of the critical fields yield the elastic coefficients, in the absence of a comprehensive theory of the elasticity of the SmZ_A one must perhaps be somewhat cautious in concluding precisely which elastic mode is being probed. Specifically, the coupling between director distortion (which also necessarily involves distortion of the polarization field) and the layer normal can be expected to play significant roles. Is this indicated by the almost thirty-fold increase in the cost of splay distortion in the SmZ_A range? To address these, future planned work includes independent measurements *via* both the bend²⁸ and twist Freedericksz transitions. This will ascertain directly the anisotropy in the elastic constants, which should better illuminate the issue of the periodic FT. Moreover, in the undistorted state for the bend transition, the layer normal will be degenerate in the plane perpendicular to the field; how this affects the transition should be highly revealing.

Conflicts of interest

There are no conflicts to declare.

Data availability

Data will be made available upon request.

Acknowledgements

This work was supported by US National Science Foundation grant DMR-2210083. We are grateful to P. Salamon and O. D. Lavrentovich for valuable discussions.

References

- 1 H. J. Deuling, Deformation of Nematic Liquid Crystals in an Electric Field, *Mol. Cryst. Liq. Cryst.*, 1972, **19**(2), 123–131. Available from: <https://www.tandfonline.com/doi/abs/10.1080/15421407208083858>.
- 2 F. Lonberg and R. B. Meyer, New Ground State for the Splay-Freedericksz Transition in a Polymer Nematic Liquid Crystal, *Phys. Rev. Lett.*, 1985, **55**(7), 718. Available from: <https://journals.aps.org/prl/abstract/10.1103/PhysRevLett.55.718>.



3 X. Chen, V. Martinez, E. Korblova, G. Freychet, M. Zhernenkov and M. A. Glaser, *et al.*, The smectic Z A phase: Antiferroelectric smectic order as a prelude to the ferroelectric nematic, *Proc. Natl. Acad. Sci. U. S. A.*, 2023, (8), 120. Available from: <https://pnas.org/doi/10.1073/pnas.2217150120>.

4 A. Ghimire, B. Basnet, H. Wang, P. Guragain, A. Baldwin, R. Twieg, *et al.*, Director-layer dynamics in the smectic-ZA phase of a ferroelectric nematic liquid crystal, *arXiv*, 2025, preprint, arXiv:2501.12541v2, DOI: [10.48550/arXiv.2501.12541](https://doi.org/10.48550/arXiv.2501.12541), Available from: <https://arxiv.org/abs/2501.12541v2>.

5 P. G. de Gennes, J. Prost, P. G. de Gennes and J. Prost, *The Physics of Liquid Crystals*, Clarendon Press, Oxford, 1993, p. 616. Available from: <https://www.amazon.ca/Physics-Liquid-Crystals-P-Gennes/dp/0198517858>.

6 S. Chandrasekhar, *Liquid Crystals*, Cambridge University Press, 2nd edn, 1993, p. 480. Available from: <https://www.amazon.com/Liquid-Crystals-S-Chandrasekhar-F-R-S/dp/052142741X>.

7 H. Nishikawa, K. Sano and F. Araoka, Anisotropic fluid with phototunable dielectric permittivity, *Nat. Commun.*, 2022, 13(1), 1–9. Available from: <https://www.nature.com/articles/s41467-022-28763-1>.

8 H. Schad, B. Scheuble and J. Nehring, On the field dependence of the optical phase difference and capacitance of nematic layers, *J. Chem. Phys.*, 1979, 71(12), 5140–5143. Available from: <https://pubs.aip.org/aip/jcp/article/71/12/5140/793006/On-the-field-dependence-of-the-optical-phase>.

9 H. Nishikawa, K. Shiroshita, H. Higuchi, Y. Okumura, Y. Haseba and Y. Shin-Ichi, *et al.*, A Fluid Liquid-Crystal Material with Highly Polar Order, *Adv. Mater.*, 2017, 29(43), 1702354. Available from: <https://onlinelibrary.wiley.com/doi/full/10.1002/adma.201702354>.

10 S. Brown, E. Cruickshank, J. M. D. Storey, C. T. Imrie, D. Pociecha and M. Majewska, *et al.*, Multiple Polar and Non-polar Nematic Phases, *ChemPhysChem*, 2021, 22(24), 2506–2510. Available from: <https://onlinelibrary.wiley.com/doi/full/10.1002/cphc.202100644>.

11 J. Thoen, G. Cordoyiannis, W. Jiang, G. H. Mehl and C. Glorieux, Phase transitions study of the liquid crystal DIO with a ferroelectric nematic, a nematic, and an intermediate phase and of mixtures with the ferroelectric nematic compound RM734 by adiabatic scanning calorimetry, *Phys. Rev. E*, 2023, 107(1), 014701. Available from: <https://journals.aps.org/pre/abstract/10.1103/PhysRevE.107.014701>.

12 J. Zhou, R. Xia, M. Huang and S. Aya, Stereoisomer effect on ferroelectric nematics: stabilization and phase behavior diversification, *J. Mater. Chem. C*, 2022, 10(22), 8762–8766. Available from: <https://pubs.rsc.org/en/content/articlehtml/2022/tc/d2tc00862a>.

13 J. C. Kemp, Piezo-Optical Birefringence Modulators: New Use for a Long-Known Effect, *J. Opt. Soc. Am.*, 1969, 59(8), 950. Available from: <https://opg.optica.org/abstract.cfm?URI=josa-59-8-950>.

14 N. A. Clark, X. Chen, J. E. MacLennan and M. A. Glaser, Dielectric spectroscopy of ferroelectric nematic liquid crystals: Measuring the capacitance of insulating interfacial layers, *Phys. Rev. Res.*, 2024, 6(1), 013195. Available from: <https://journals.aps.org/prresearch/abstract/10.1103/PhysRevResearch.6.013195>.

15 L. Leger, Walls in Nematics, *Mol. Cryst. Liq. Cryst.*, 1973, 24(1–2), 33–44. Available from: <https://www.tandfonline.com/doi/abs/10.1080/15421407308083386>.

16 T. Uchida and Y. Takahashi, New Method to Determine Elastic Constants of Nematic Liquid Crystal From C-V Curve, *Mol. Cryst. Liq. Cryst.*, 1981, 72(4), 133–137. Available from: <https://www.tandfonline.com/doi/abs/10.1080/01406568108084049>.

17 F. Brochard, Backflow Effects in Nematic Liquid Crystals, *Mol. Cryst. Liq. Cryst.*, 1973, 23(1–2), 51–58. Available from: <https://www.tandfonline.com/doi/abs/10.1080/15421407308083360>.

18 L. J. Yu and A. Saupe, Observation of a biaxial nematic phase in potassium laurate-1-decanol-water mixtures, *Phys. Rev. Lett.*, 1980, 45(12), 1000–1003.

19 J. S. Patel and H. Yokoyama, Continuous anchoring transition in liquid crystals, *Nature*, 1993, 362(6420), 525–527.

20 K. Van Le, M. Mathews, M. Chambers, J. Harden, Q. Li and H. Takezoe, *et al.*, Electro-optic technique to study biaxiality of liquid crystals with positive dielectric anisotropy: The case of a bent-core material, *Phys. Rev. E: Stat., Nonlinear, Soft Matter Phys.*, 2009, 79(3), 030701. Available from: <https://pre.aps.org/abstract/PRE/v79/i3/e030701>.

21 T. Ostapenko, C. Zhang, S. N. Sprunt, A. Jákli and J. T. Gleeson, Magneto-optical technique for detecting the biaxial nematic phase, *Phys. Rev. E: Stat., Nonlinear, Soft Matter Phys.*, 2011, 84(2), 021705. Available from: <https://link.aps.org/doi/10.1103/PhysRevE.84.021705>.

22 C. Zhang, S. Chakraborty, T. Ostapenko, S. Sprunt, A. Jákli and J. T. Gleeson, Biaxial nematic order induced by smectic fluctuations, *Phys. Rev. E: Stat., Nonlinear, Soft Matter Phys.*, 2012, 86, 2.

23 Y. A. Nastishin, R. D. Polak, S. V. Shlyanovskii, V. H. Bodnar and O. D. Lavrentovich, Nematic polar anchoring strength measured by electric field techniques, *J. Appl. Phys.*, 1999, 86(8), 4199–4213. Available from: <https://pubs.aip.org/aip/jap/article/86/8/4199/487811/Nematic-polar-anchoring-strength-measured-by>.

24 T. J. Scheffer and J. Nehring, Accurate determination of liquid-crystal tilt bias angles, *J. Appl. Phys.*, 1977, 48(5), 1783–1792. Available from: <https://pubs.aip.org/aip/jap/article/48/5/1783/8215/Accurate-determination-of-liquid-crystal-tilt-bias>.

25 J. T. Gleeson, New ways to produce and measure low pre-tilt angles, *Liq. Cryst.*, 1996, 20, 4.

26 L. Paik and J. V. Selinger, *Flexoelectricity versus Electrostatics in Polar Nematic Liquid Crystals*, *arXiv*, 2024, preprint, arXiv:2408.10347, DOI: [10.48550/arXiv.2408.10347](https://doi.org/10.48550/arXiv.2408.10347), Available from: <https://arxiv.org/pdf/2408.10347.pdf>.



27 S. M. Shamid, S. Dhakal and J. V. Selinger, Statistical mechanics of bend flexoelectricity and the twist-bend phase in bent-core liquid crystals, *Phys. Rev. E*, 2013, **87**(5), 052503. Available from: <https://journals.aps.org/pre/abstract/10.1103/PhysRevE.87.052503>.

28 B. Basnet, S. Paladugu, O. Kurochkin, O. Buluy, N. Aryasova and V. G. Nazarenko, *et al.*, Periodic splay Fréedericksz transitions in a ferroelectric nematic, *Nat. Commun.*, 2025, **16**(1), 1–13. Available from: <https://www.nature.com/articles/s41467-025-55827-9>.

